Two Fluid Numerical Studies of Interchange Modes in Spheromak Equilibria

Eric Howell, Carl Sovinec
University of Wisconsin-Madison

Sherwood Meeting
Seattle, Washington
April 19-21, 2010

THE UNIVERSITY of WISCONSIN MADISON

NIMROD
Non-Ideal MHD with Rotation
Open Discussion Project

Introduction and Motivation

Outline of poster

- Linear calculations of both resistive and ideal interchange modes in a cylindrical spheromak
- Linear calculations of ideal interchange modes in a realistic “tuna-can” spheromak
- Preliminary nonlinear simulations of interchange mode in “tuna-can” spheromak

Large catastrophic interchange modes have been reported during the decay phase in both CTX and SSPX.

- In CTX, prior to the crash the Mercier stability limit is greatly exceeded, by as much as x40.
  - In SSPX, the spheromak recovers and T_e evolves with the Mercier limit.
- In SSPX the instability is only reported in a modified operating scenario when a large background vertical field is applied.
- In “normal” SSPX operation the sustainment pulse prevents low order rational surfaces from appearing, and catastrophic interchange modes are not observed.

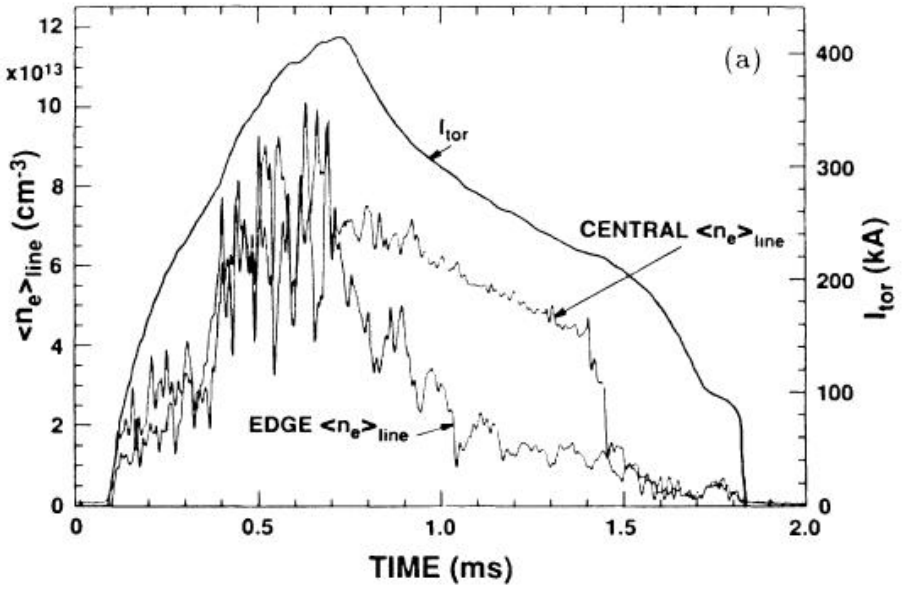

Around 1.4 ms a pressure driven interchange mode is observed in CTX. The core density drops by x4 in ~20 mus [F. J. Wysocki et al, PRL 61, 1988].

Resistive MHD simulations using NIMROD have reproduced many aspects of SSPX discharges but often underestimate peak temperature.

- In the best preforming discharges, NIMROD simulations under-predict peak temperatures by as much as ~40%.
- Stability calculations with NIMROD of decaying spheromak profiles exhibit interchange behavior.
- Two fluid physics, not included in the resistive MHD model, introduce drifts which act to reduce the growth rate and can completely stabilize interchange instabilities.
- Under-predicting the stability of these modes would over-predict the transport and thus under-predict T_e.
- Kinetic effects due to low collisionality may also explain the difference. [J. Ji et al, POP 16, 2009]

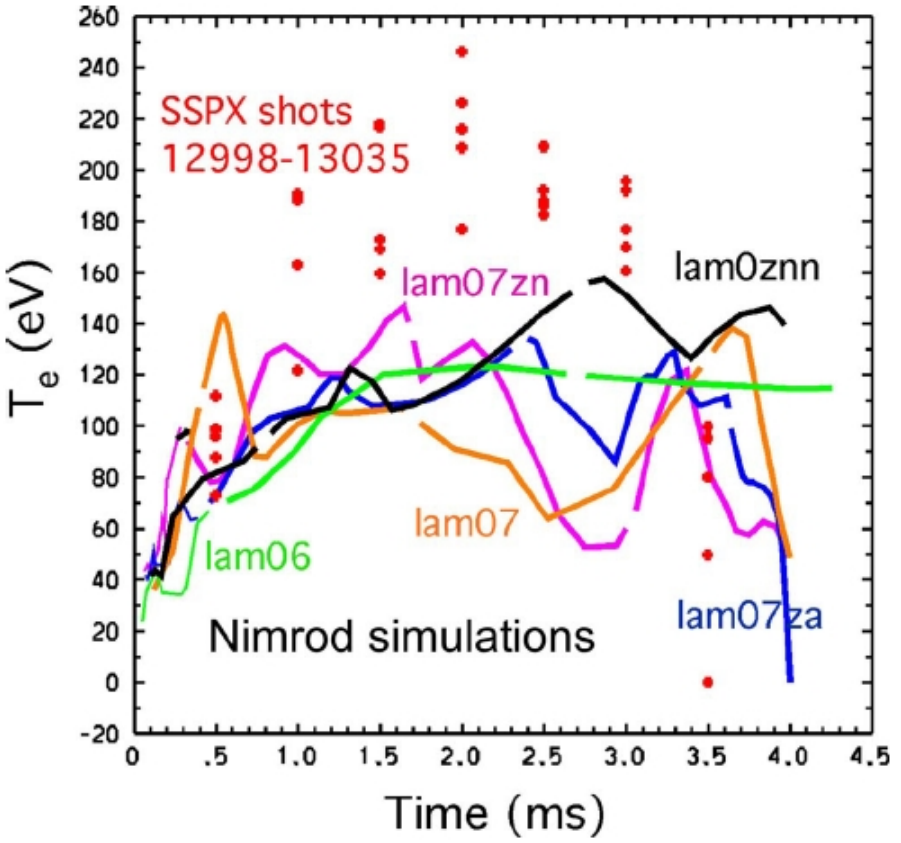

Hooper et al, POP 15, 2008

Numerical calculations are needed for geometry and profiles of spheromaks.

- Linear theory, including Hall and gyro-viscous terms, for the localized g-mode is sufficiently complex with arbitrary profiles in slab geometry. [P. Zhu et al, PRL 101, 2008]
- Analytics are further complicated by incorporating realistic effects from complex magnetic geometries, spatial variation of the mode, and toroidal geometry.
- NIMROD has two-fluid modeling necessary for assessing stability.
- High-order finite element representation enables accurate computation with arbitrary cross-section geometry.

The NIMROD code evolves a fluid model using the following set of equations.

$$\rho\left(\frac{\partial \vec{V}}{\partial t}+\vec{V}\cdot\nabla\vec{V}\right)=\vec{J}\times\vec{B}-\nabla P-\nabla\cdot\Pi_i$$

$$\Pi_i=-\rho\nu_{iso}W+f_{gv}\Pi_{gv}$$

Gyro-viscous stress tensor

$$\Pi_{gv}=\frac{m_i P_i}{4eB}\left[\hat{b}\times W\cdot(I+3\hat{b}\hat{b})-(I+3\hat{b}\hat{b})\cdot W\times\hat{b}\right]$$

$$\frac{\partial n}{\partial t}+\nabla\cdot(n\vec{V})=\nabla\cdot(D\nabla n-D_h\nabla\nabla^2 n)$$

$$\frac{n}{\gamma-1}\left(\frac{\partial T_\alpha}{\partial t}+\vec{V}_\alpha\cdot\nabla T_\alpha\right)=-P_\alpha\nabla\cdot\vec{V}_\alpha-\nabla\cdot\vec{q}_\alpha+Q_\alpha$$

2 fluid corrections to Ohm's law

$$\frac{\partial \vec{B}}{\partial t}=-\nabla\times(\eta\vec{J}-\vec{V}\times\vec{B})-\nabla\times\left[\frac{1}{ne}(\vec{J}\times\vec{B}-T_e\nabla n)+\mu_0 d_e^2\frac{\partial \vec{J}}{\partial t}\right]+k_{divb}\nabla\nabla\cdot\vec{B}$$

$$\nabla\times\vec{B}=\mu_0\vec{J}$$

- W is the traceless rate of strain tensor
- 2-fluid corrections in Faraday's law include the Hall term, electron pressure, and electron inertia.
- Artificial particle diffusivity keeps noise from accumulating in the density profile.
- The last term in the magnetic evolution equation is used to control the magnetic divergence error.

Linear Calculations in Cylindrical Spheromak equilibria

A family of cylindrical spheromak equilibria are constructed using a previously studied analytic profile [J. DeLucia *et al*, Phys. Fluids **27**(1984)].

$$q = \frac{rB_z}{RB_\theta} = q_0\left(1 - r^2\right)$$

$$\frac{dp}{dr} = -\alpha \frac{r\,B_z^2}{8}\left(\frac{dq}{dr}\frac{1}{q}\right)^2$$

$$\mu_0 \frac{dp}{dr} + \frac{1}{2}\frac{dB^2}{dr} + \frac{dB_\theta}{r}\frac{d\left(rB_\theta\right)}{dr} = 0$$

- Different equilibria are used to study the stabilization of ideal interchange and resistive interchange modes in similar equilibrium.
- The factor of α in the pressure derivative determines the stability of the equilibrium to Suydam interchange modes.
  - $\alpha > 1$ is ideally unstable
  - $0 < \alpha < 1$ is ideally stable but resistively unstable
  - $\alpha < 0$ is stable

Significant Hall stabilization is observed for a m=1 resistive interchange mode.

- An isothermal equilibrium is used with q_0=0.8, α = 0.7, n=2, S=10^5, L=2π, a = 1, β_0 =0.07, and warm ions (P_i=P_e).
- Calculations are performed using the two fluid Ohm's law but neglecting gyro-viscosity.
- A 80% reduction in growth rate is calculated at Λ=1/(ω_{ci} τ_A)=0.10. Here the real frequency is approximately twice the MHD growth rate.
- Using a similar equilibrium with cold ions J. DeLucia et al, report complete stabilization for $\Lambda \approx 0.15$.
- Complete Stabilization has not been confirmed.

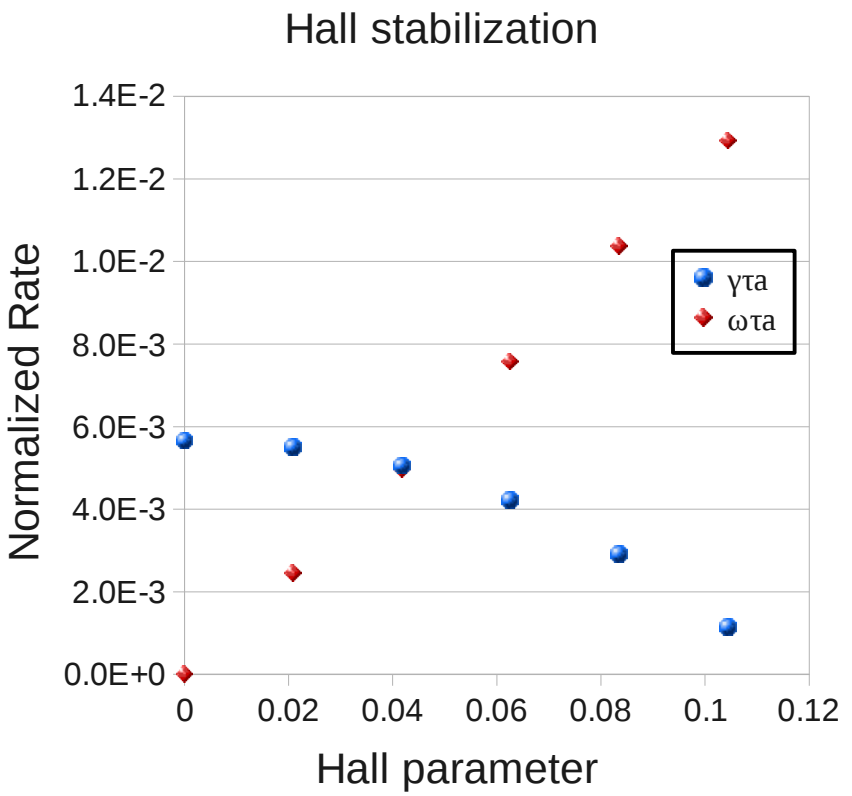

The Hall term alters the phase difference between V_r and V_θ and introduces oscillations in the mode structure.

(The two lines in each plot are along radii separated by 90 degrees).

Λ=0

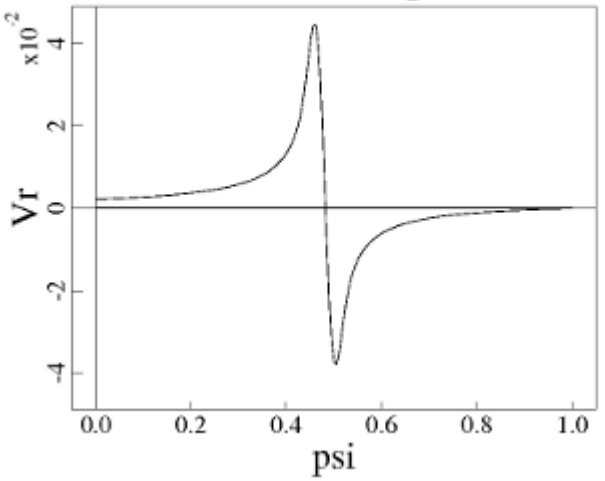

Λ=0.04

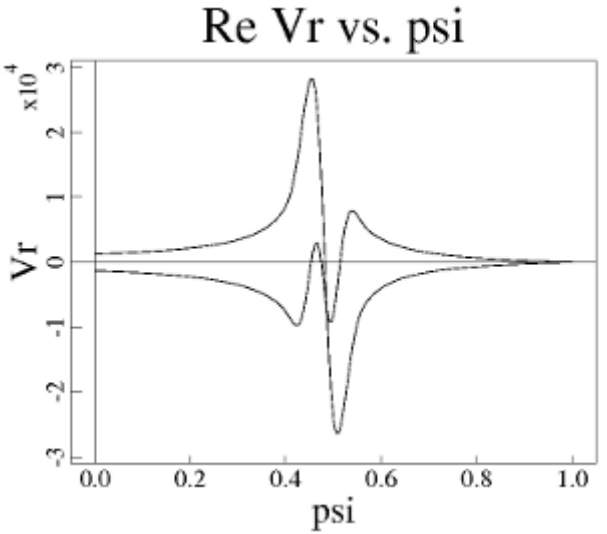

Λ=0.08

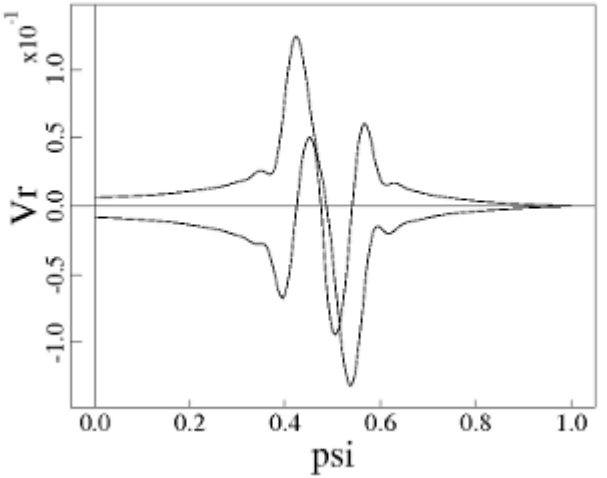

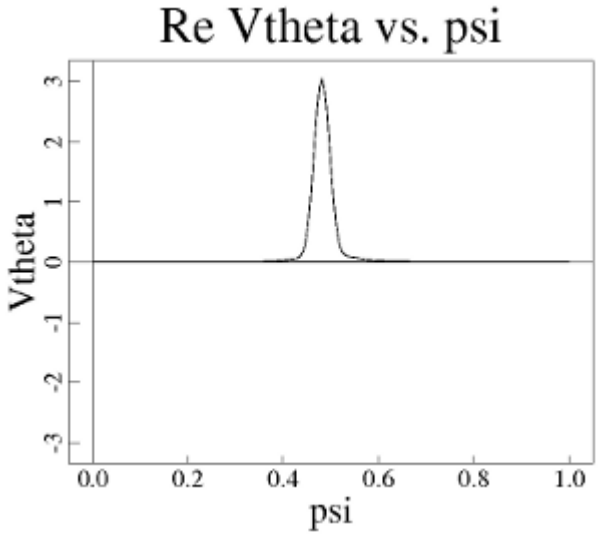

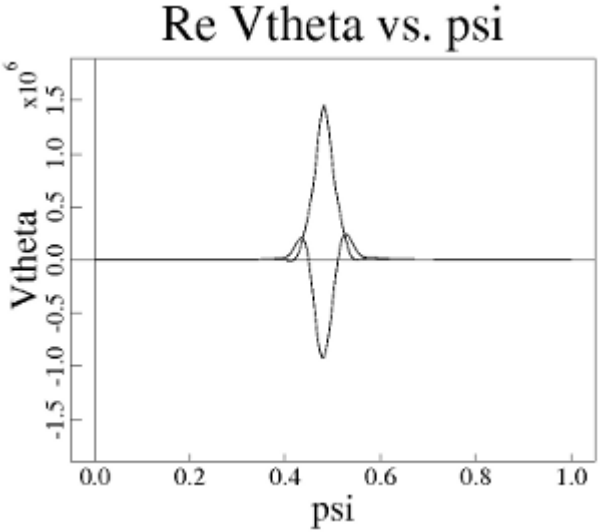

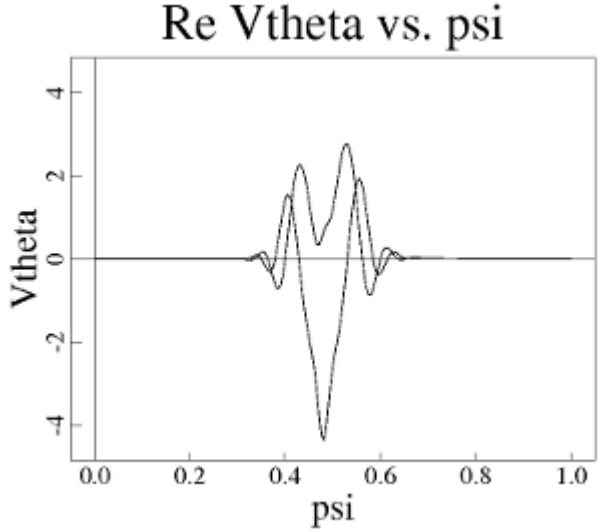

The two fluid stabilization in calculations using gyro-viscosity with the MHD Ohm's law is weaker.

- The strength of the gyro-viscous stress is increased by reducing the electron charge.
- The growth rate of the mode is reduced at higher Hall parameters.
- A 32% reduction in growth rate is calculated at Λ=0.125.
- The real frequency of the mode peaks around $\Lambda \approx 0.1$ and then decreases as the Hall parameter is further increased.
- In calculations using both the two fluid Ohm's law and gyro-viscosity the real frequencies and the growth rates of the mode are decreased relative to calculations using the two fluid Ohm's law without the gyro-viscosity.

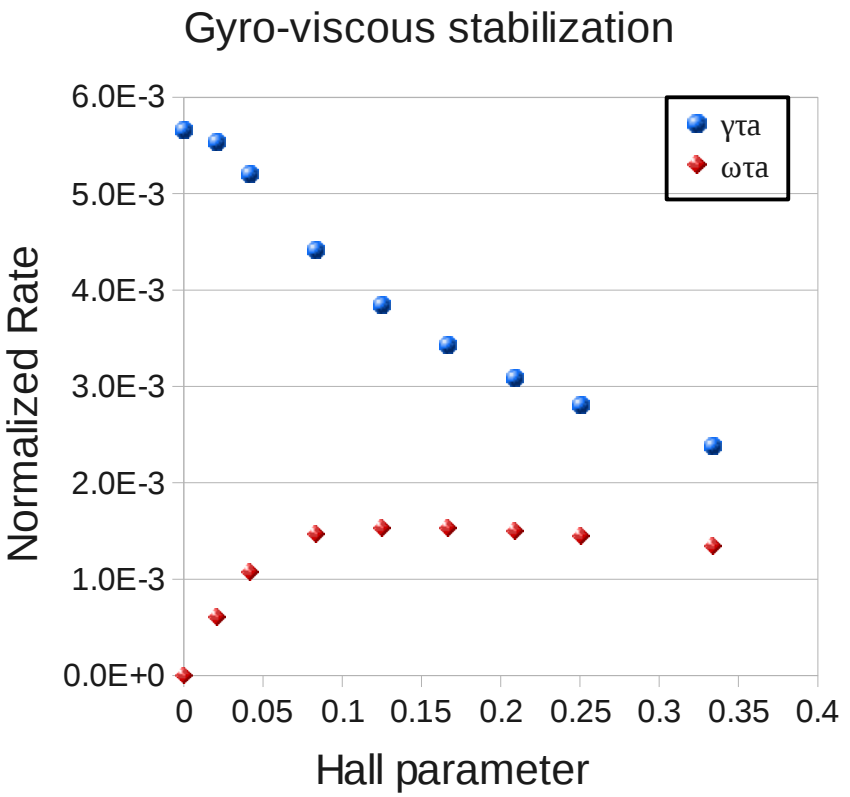

Modifications to the MHD mode structure created due to gyro-viscosity are most pronounced in V_θ.

(The two lines in each plot are along radii separated by 90 degrees).

Λ=0

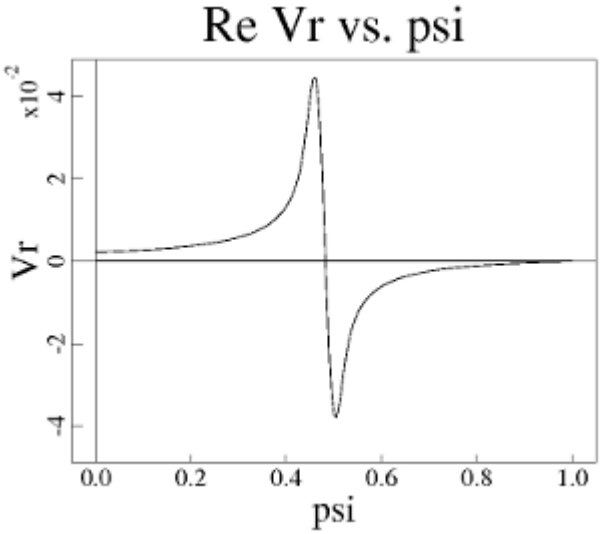

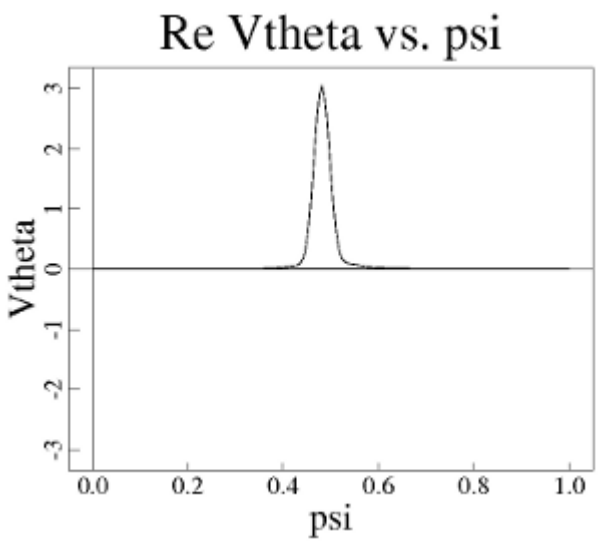

Λ=0.125

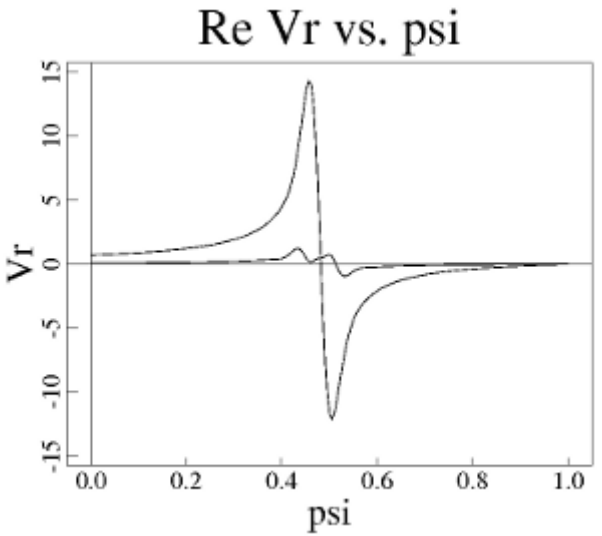

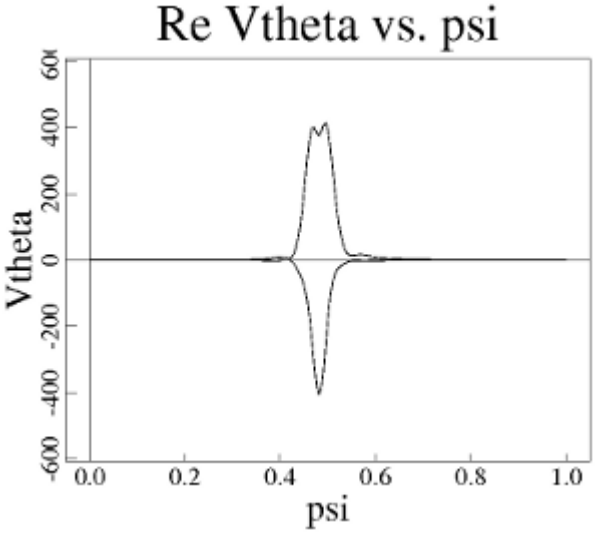

Λ=0.25

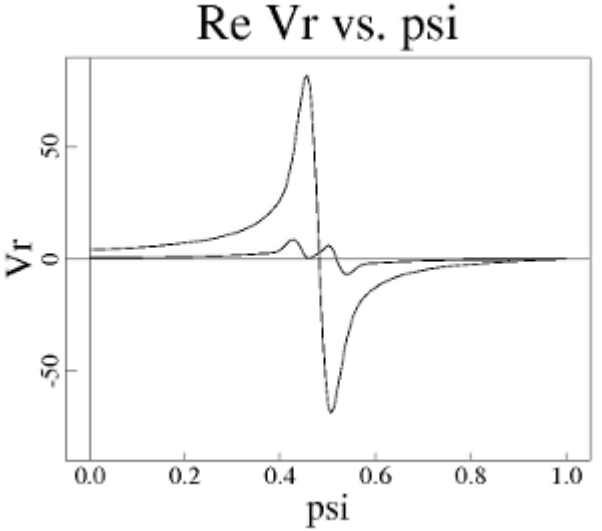

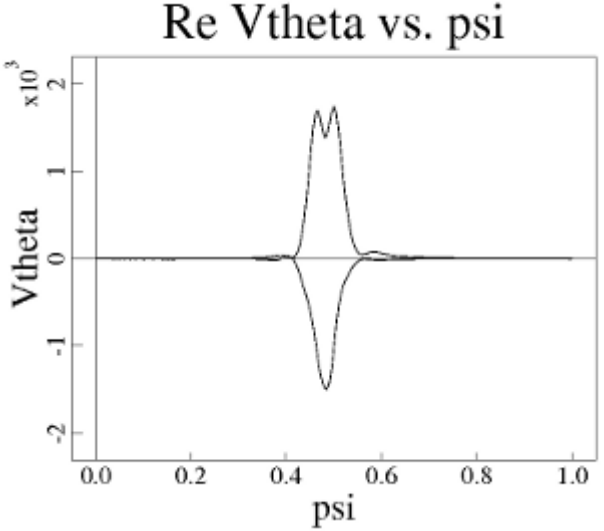

Calculations performed with a uniform equilibrium number density show qualitative agreement with uniform temperature calculations.

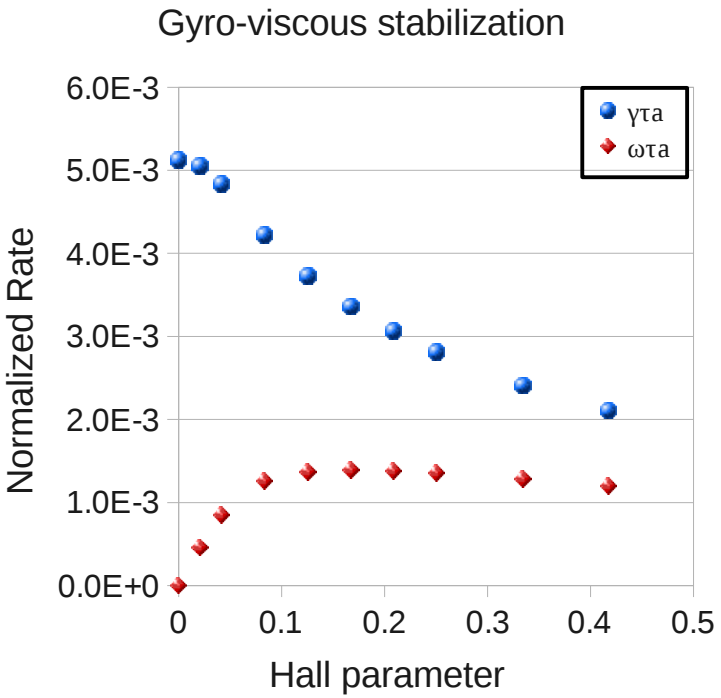

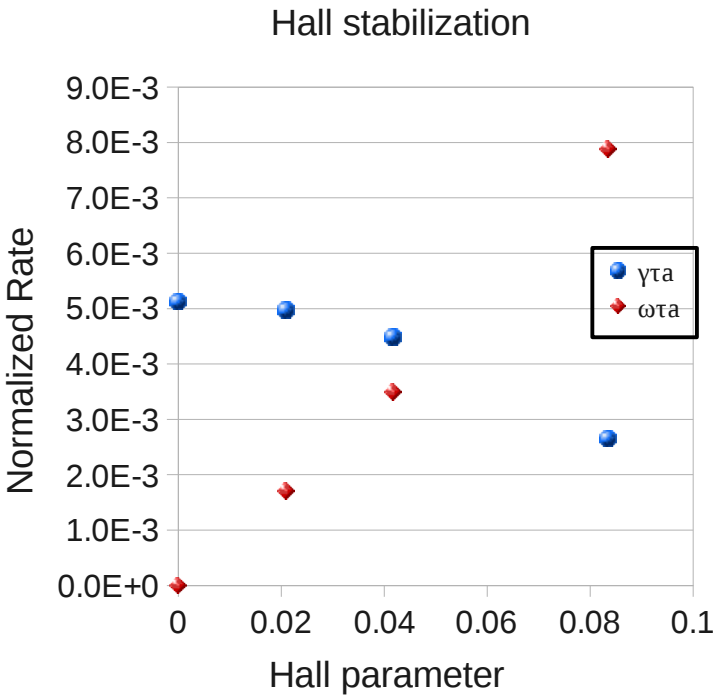

- MHD calculations using uniform density yield growth rates are 9% smaller than calculations with uniform temperature due to increased inertia at the rational surface.
- All remaining calculations are preformed using uniform number density profiles.
- Complete Hall stabilization has not been confirmed.

Modes near the stability threshold have tearing parity.

α =0.7

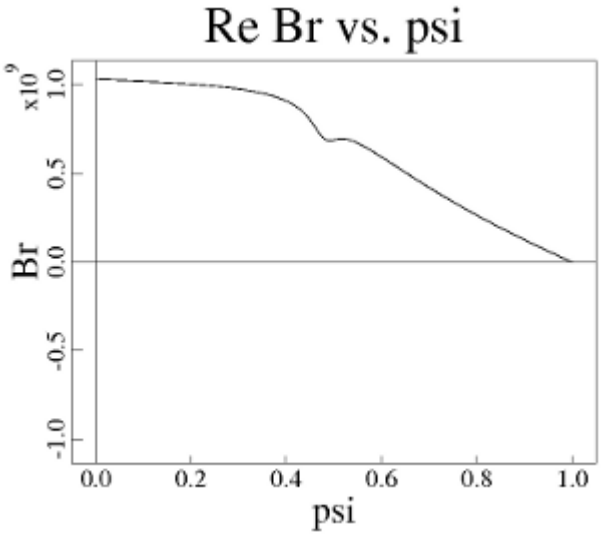

α =1.2

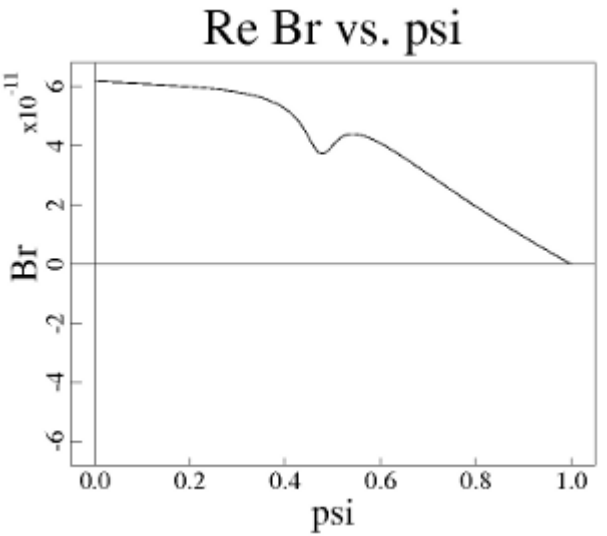

α =2.0

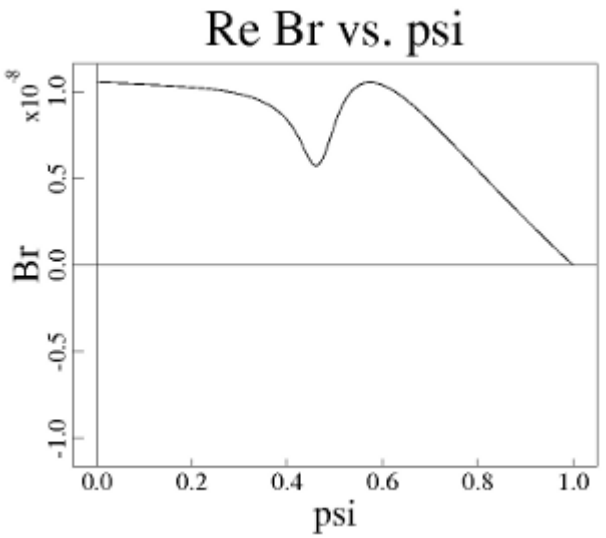

α =5.0

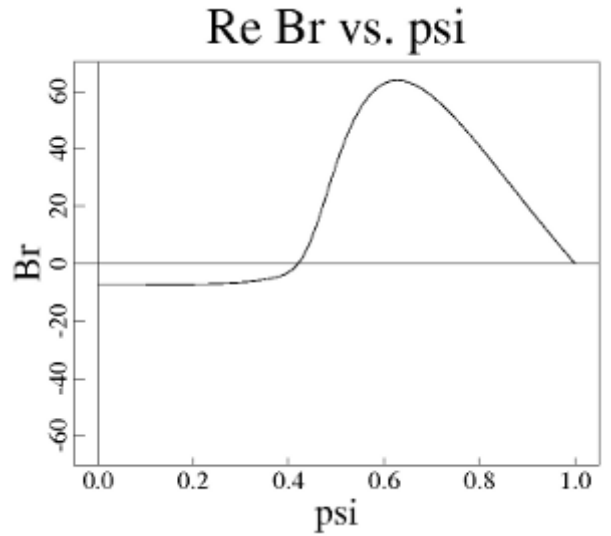

Both stabilization mechanisms are less effective in reducing the growth rate for ideally unstable equilibria.

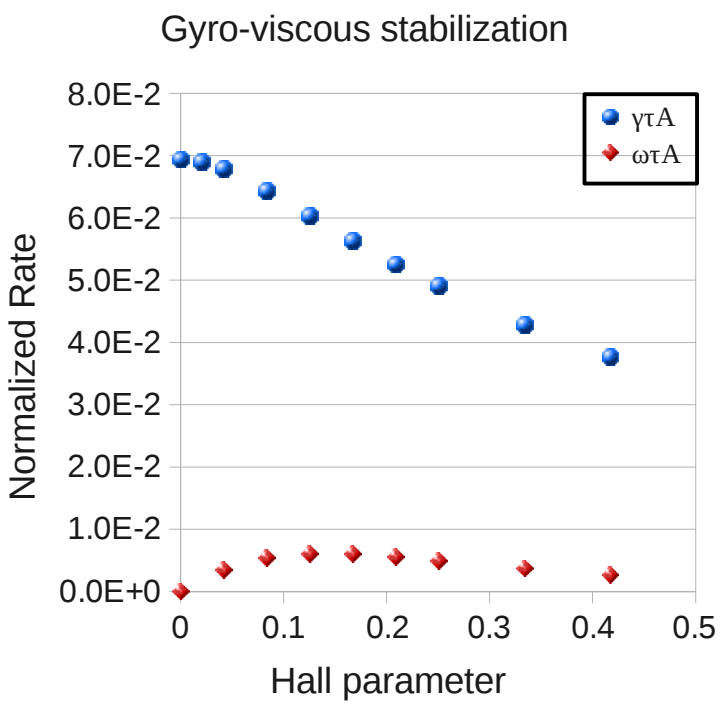

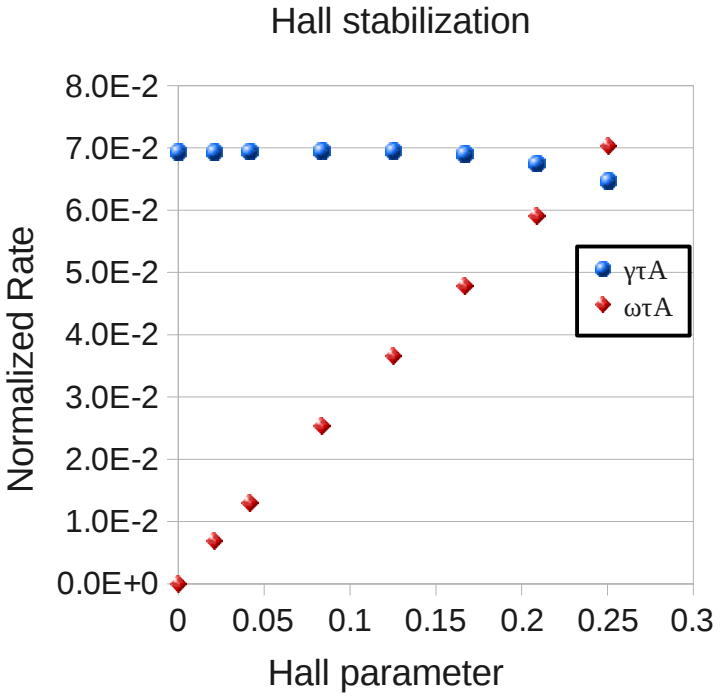

- Calculations are performed on an equilibrium with α=5.0 and β_0 =0.8.
- The Hall physics has a negligible effect of the growth rate for moderate Hall parameters, where the real frequency of the mode is much less than the growth rate.
- Gyro-viscosity produces a noticeable decrease in growth rate, but the real frequency of the mode is small relative to the growth rate.

At Λ=0.125 the Hall physics and the gyro-viscosity modify the ideal MHD V_r and V_θ differently.

(The two lines in each plot are along radii separated by 90 degrees).

MHD

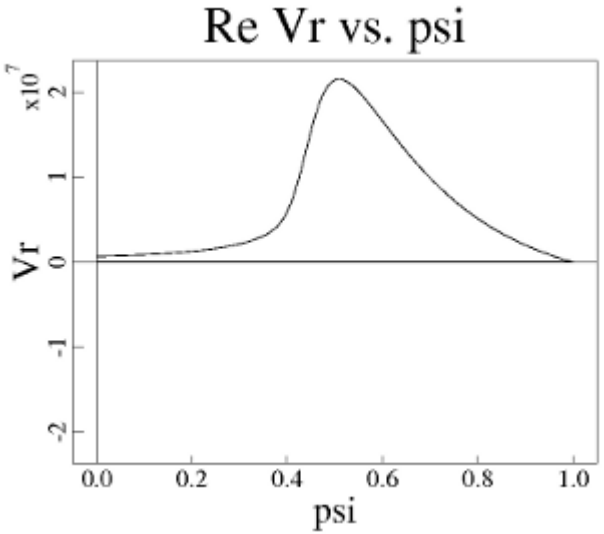

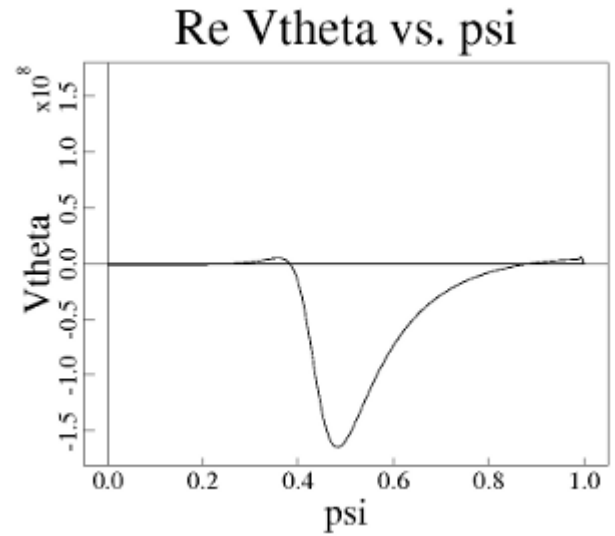

Gyro-Viscosity

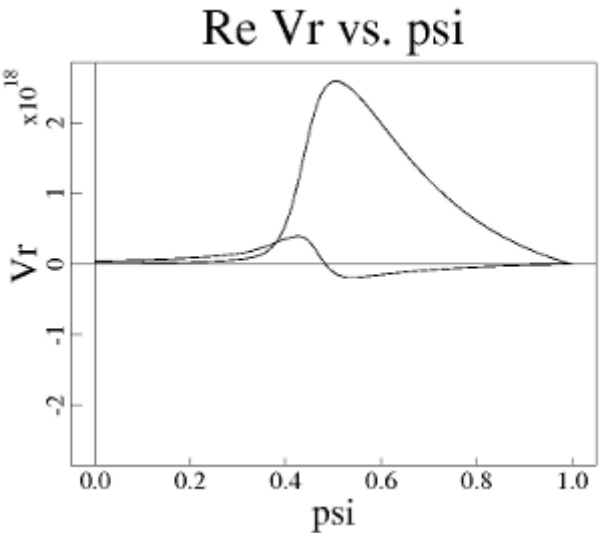

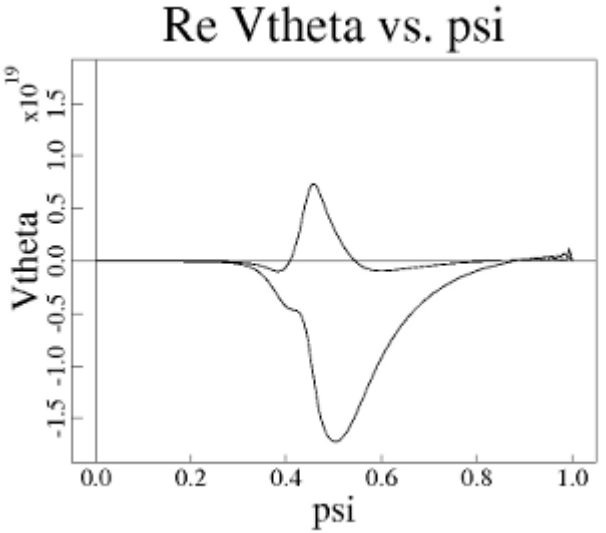

Hall

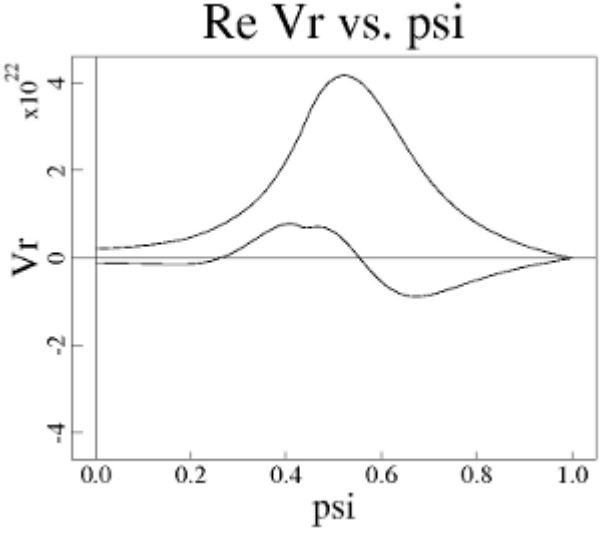

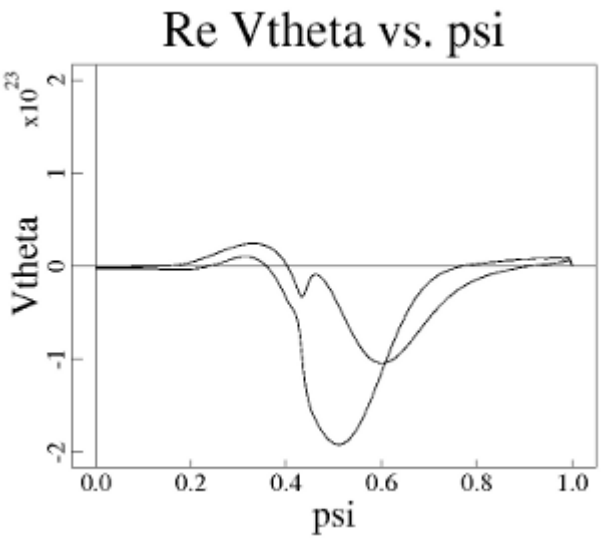

Linear Calculations in the realistic tuna-can spheromak

A second spheromak equilibrium representative of decaying spheromaks in SSPX is generated using NIMEQ.

- Toroidal geometry is used in a cylindrical domain with a centrally peaked pressure profile and slightly peaked current profiles.
- The equilibrium is tailored to included the q=2/3 rational surface.
- For both linear and nonlinear calculations the following parameters are used.
- $S=10^4$
- $\beta=6.72\%$
- $Pm=0.5$
- $\tau_A=1.64\times10^{-7}s$

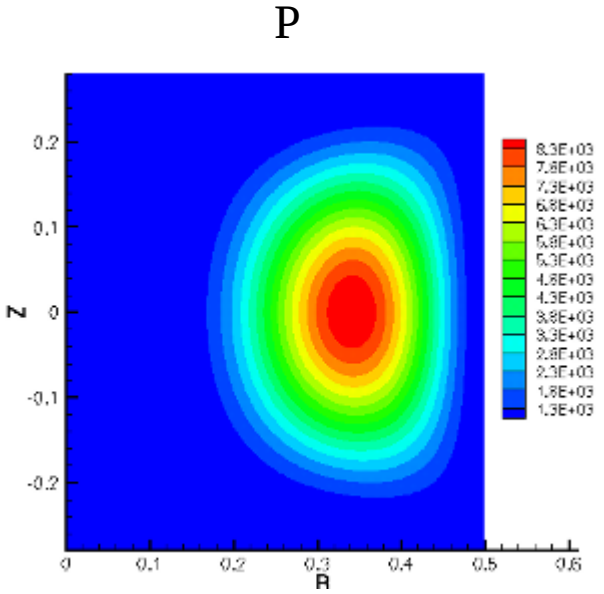

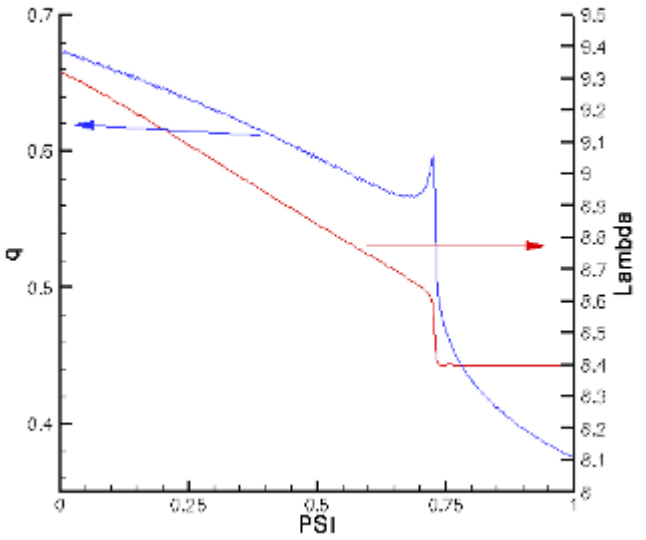

Both stabilization mechanisms have a comparable effect on the growth rate of the n=3, m=2 mode in the realistic spheromak equilibrium.

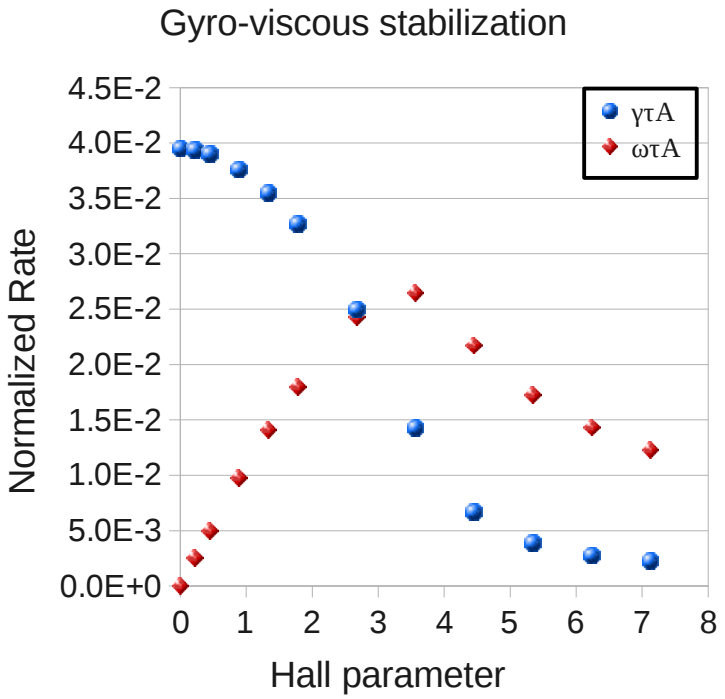

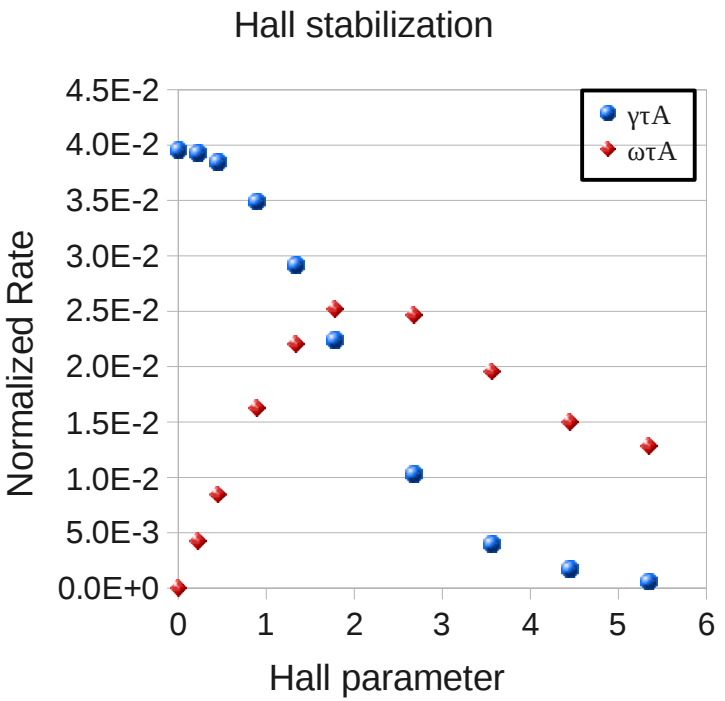

- Unrealistically large Hall parameters are needed before significantly stabilization is observed.
- The real frequencies calculated using gyro-viscosity with the MHD Ohm's law are comparable to those calculated when the two fluid Ohm's law is used without gyro-viscosity.
- The reduction in growth rate due to Hall physics is greater than the reduction due to the gyro-viscosity.

The growth rates calculated using the full model are approximately equal to the growth rates calculated when the two fluid Ohm's law is used without gyro-viscosity.

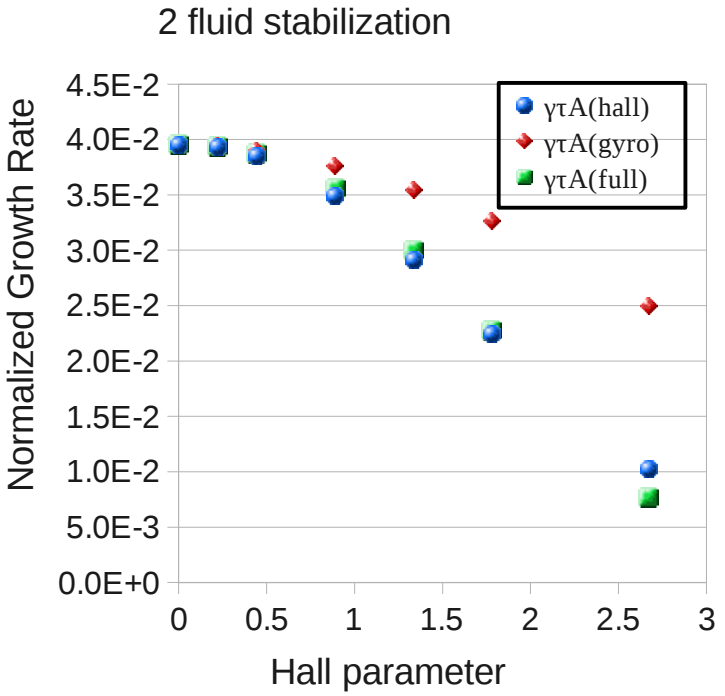

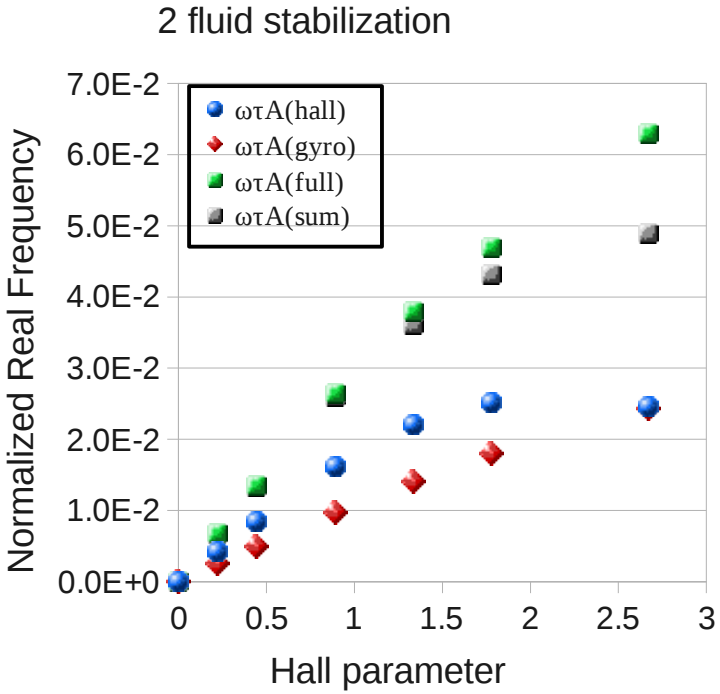

- At small Hall parameters, the real frequency calculated using the full model is approximately the sum of the frequencies calculated using two fluid Ohm's law and and gyro-viscosity independently.
- The Hall physics interacts synergistically with the gyro-viscosity increasing the real frequency at large Hall parameters.

In agreement with the n=3 mode, both stabilizing mechanisms have a comparable effect on the growth rate of the n=5, m=3 mode.

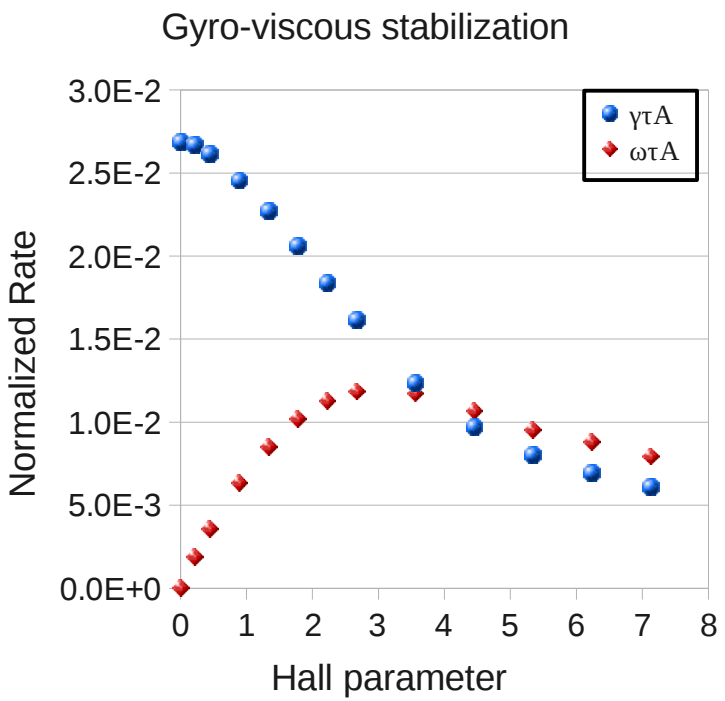

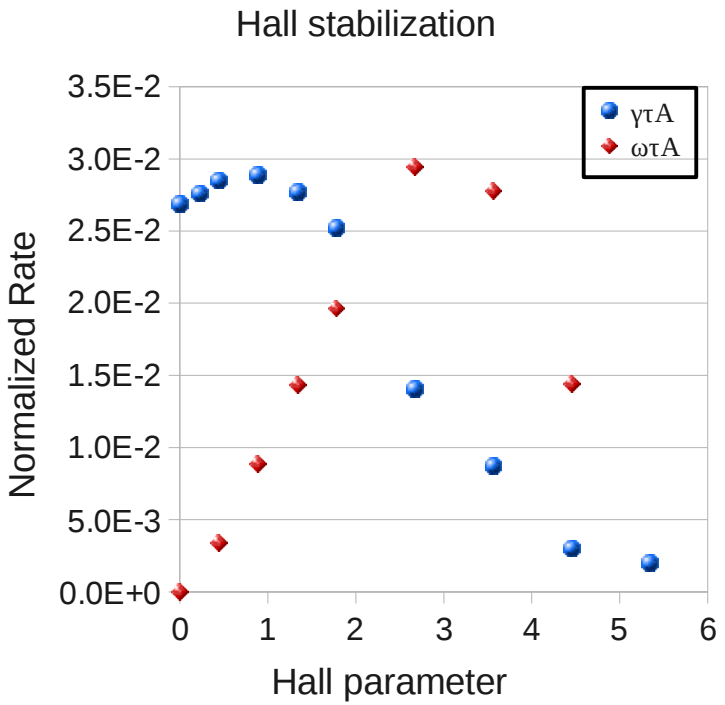

- The MHD growth rate of n=5 mode, located near the last closed flux surface, is weaker than the n=3 mode, located near the magnetic axis.
- At small Hall parameters, the Hall physics enhances the n=5 growth rate but transitions to reducing the growth rate at large enough Hall parameter.

Nonlinear simulations of interchange modes in tuna-can spheromak equilibrium.

The n=3 mode is the dominate mode in MHD nonlinear simulations with 6 toroidal Fourier modes (n=0-5).

- The simulations evolve nonlinear perturbations from the axisymmetric equilibrium used in linear computations.
- The n=3 mode is the most linearly unstable mode, and is evolved from its linear phase first.
- Late in the MHD simulation, the perturbed magnetic energy saturates around $b/B_0 \approx 2.0\%$.
- The temperature evolution in these simulations is mostly adiabatic.
- The instability reduces the pressure gradient, reducing the pressure in the core and and increasing it near the edge.
- The instability increases the number density in the core and reduces the temperature .

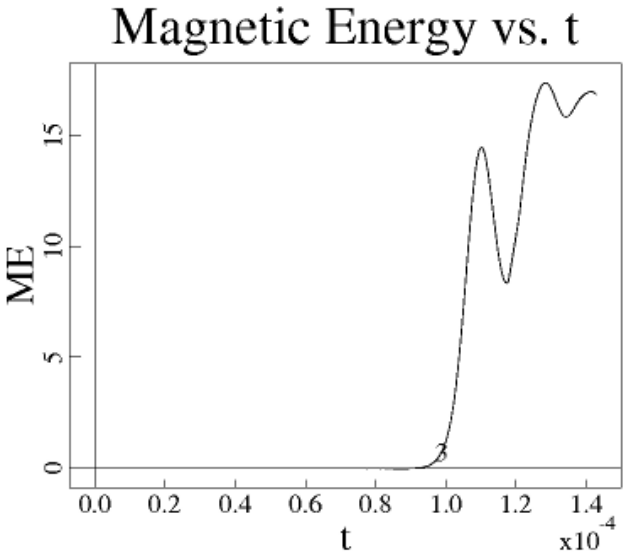

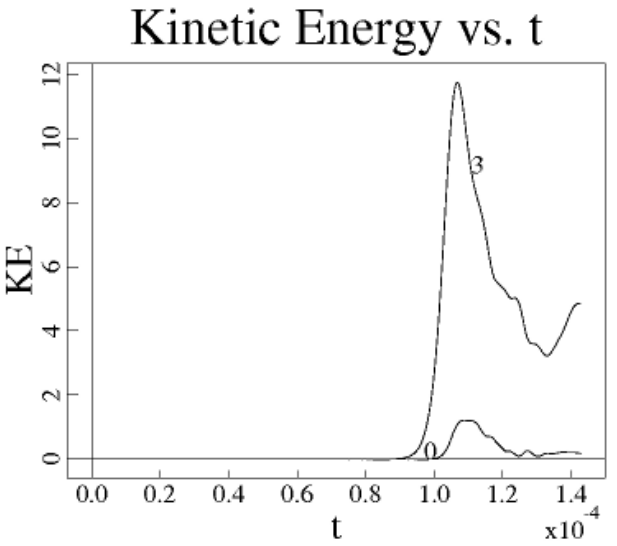

As the instability evolves, lobes of high pressure develop near the edge and the pressure in the core is reduced.

t=0.1008ms

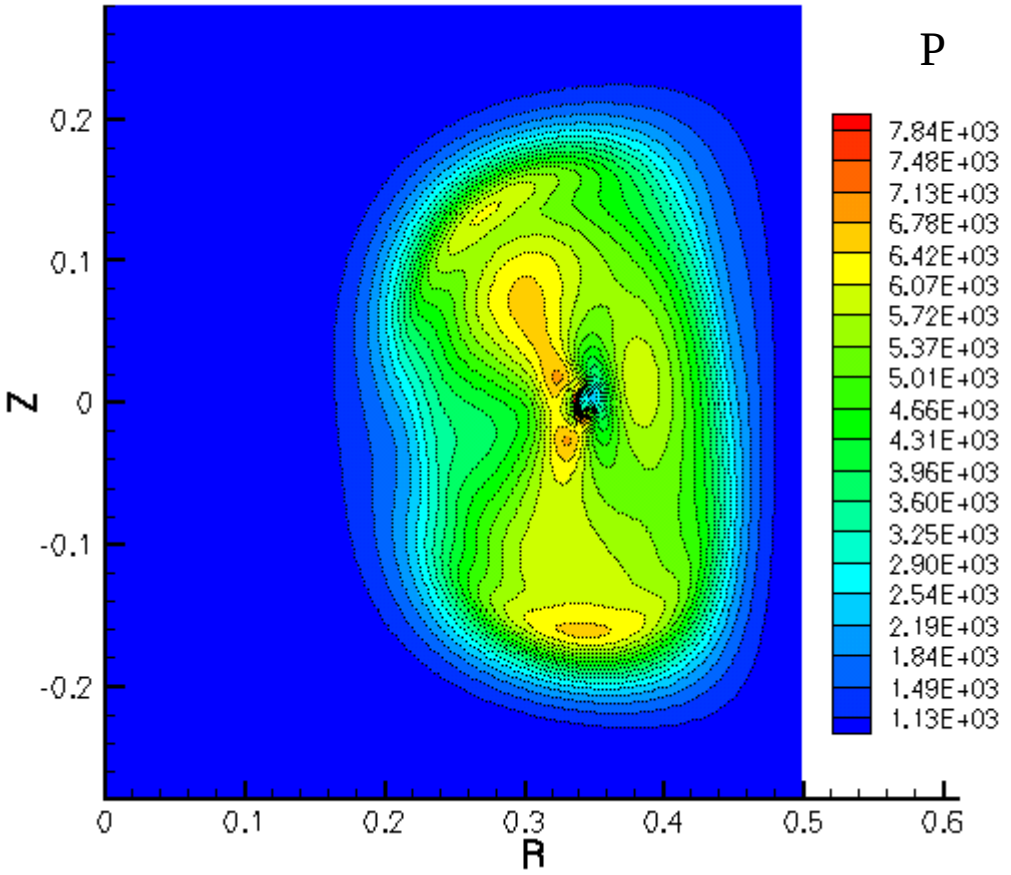

t=0.1428ms

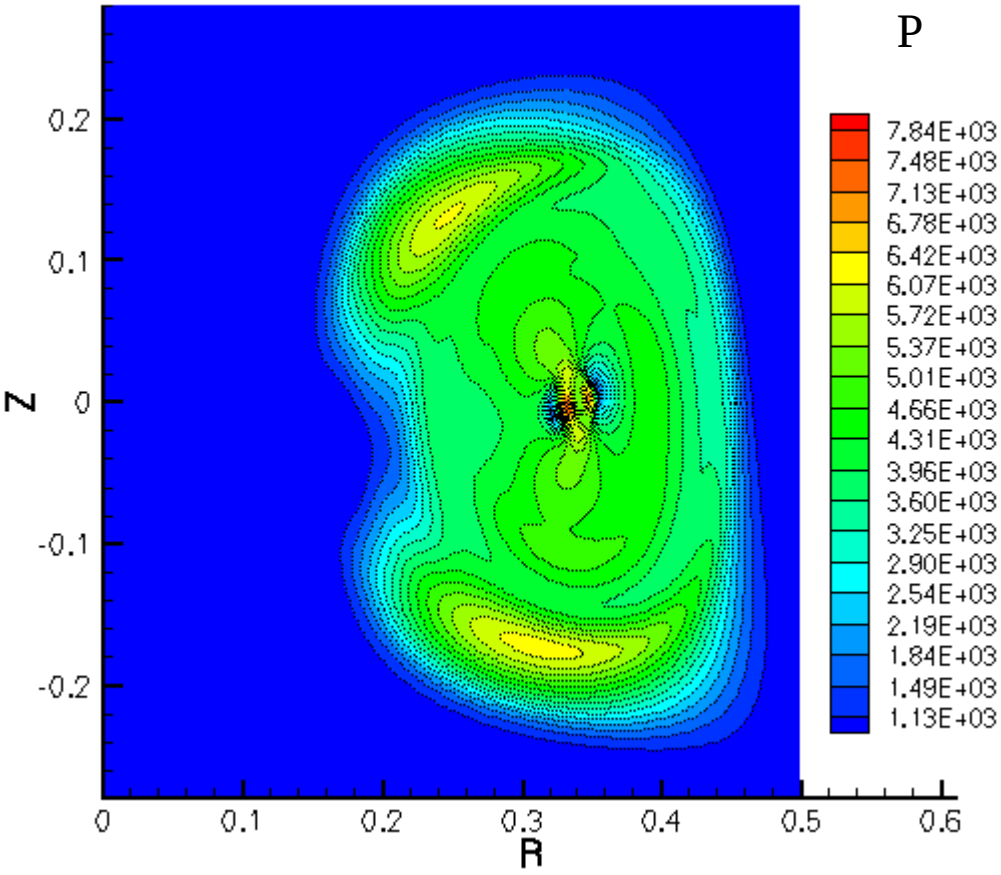

Nested flux surfaces persist in the lobes through the highly nonlinear stage of the MHD simulation. Flux surfaces in the core are created and then destroyed during oscillations of high and low perturbed magnetic energy.

t=0.1008ms

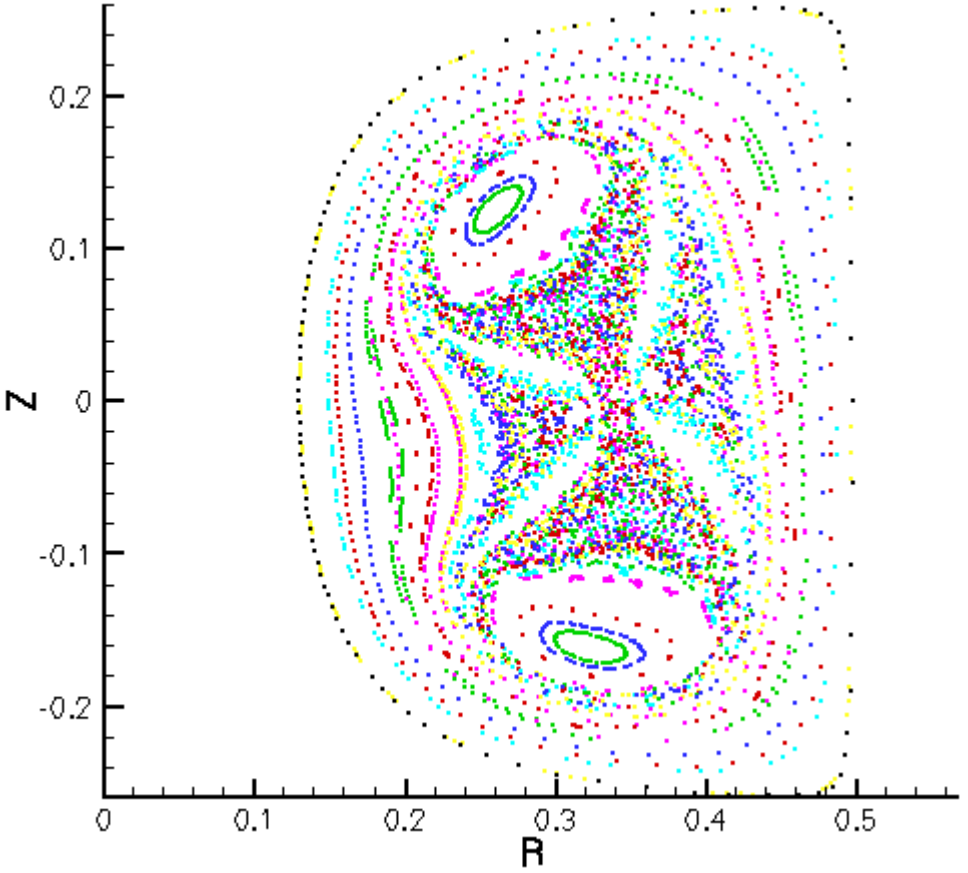

t=0.1428ms

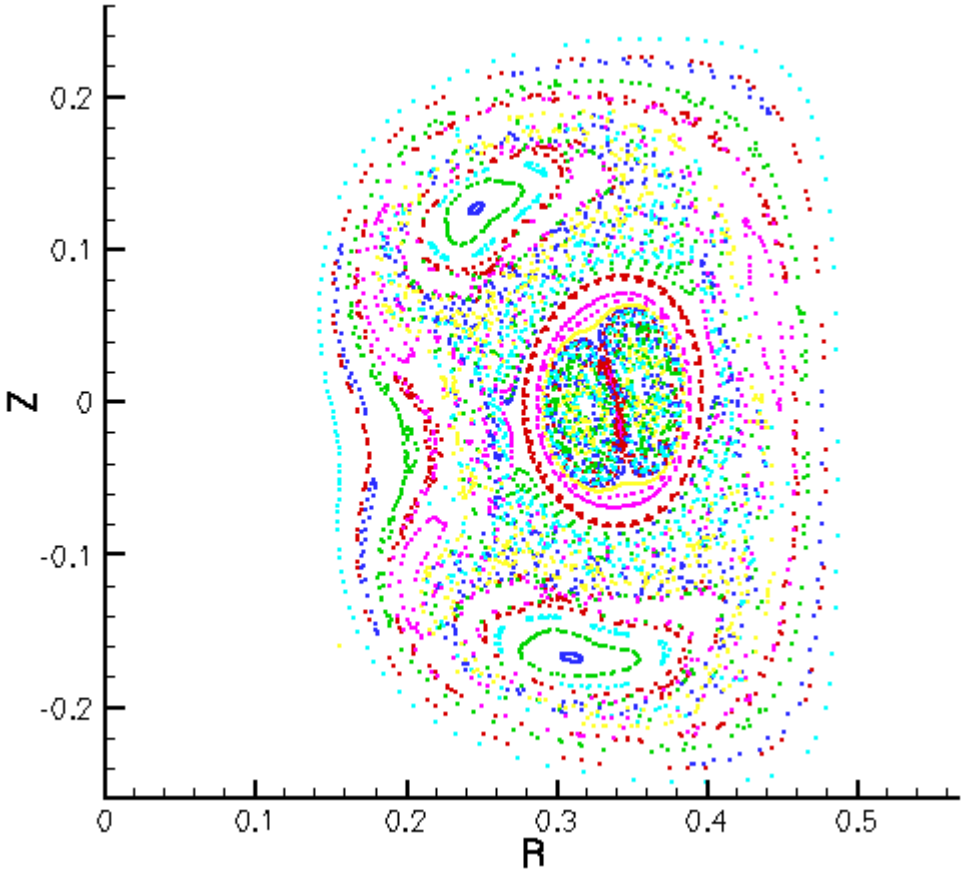

Two fluid effects reduce the final perturbed magnetic energy of the interchange mode.

- Two fluid simulations include both the two fluid Ohm's law and the gyro-viscous stress, and use a realistic Hall parameter.
- The MHD simulation is used to seed the instability, and two fluid physics are turned on around 98 μs into the simulation.
- Initially the simulation using the two-fluid model peaks at a higher perturbed magnetic energy than the MHD simulation.
- The perturbed magnetic energy near the end of the simulation drops to $b/B_0 \approx 1.6\%$.
- At the end of the simulation higher order modes appear, and more toroidal resolution is needed.
- Both the n=0 and n=3 perturbed kinetic energies are larger when two fluid effects are included.

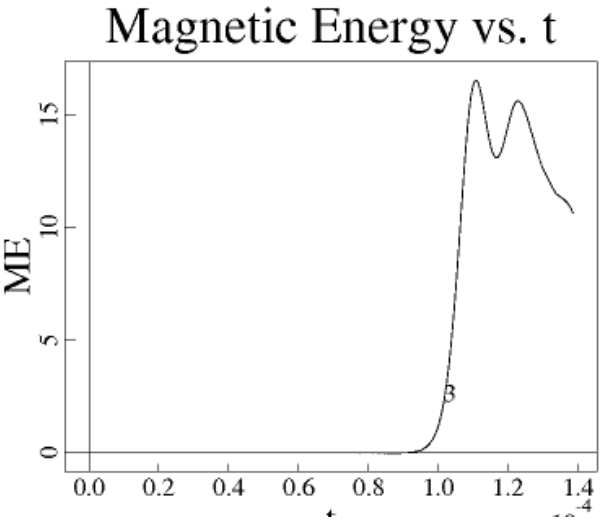

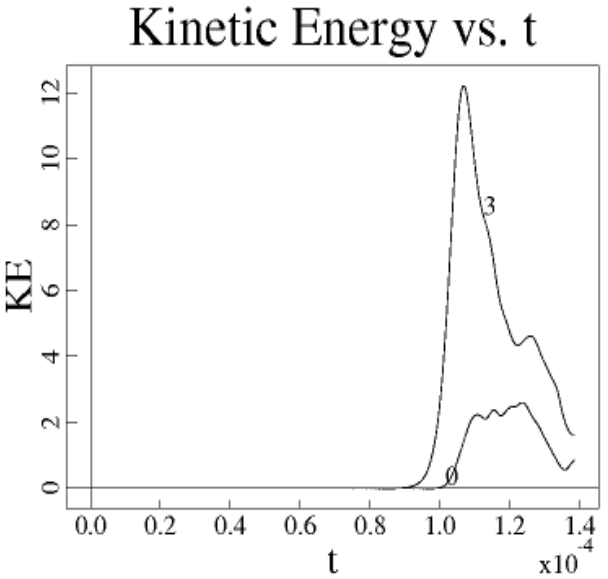

The two fluid effects help smooth out the fine scale pressure structures that develop in the core in MHD simulations.

t=0.10089ms

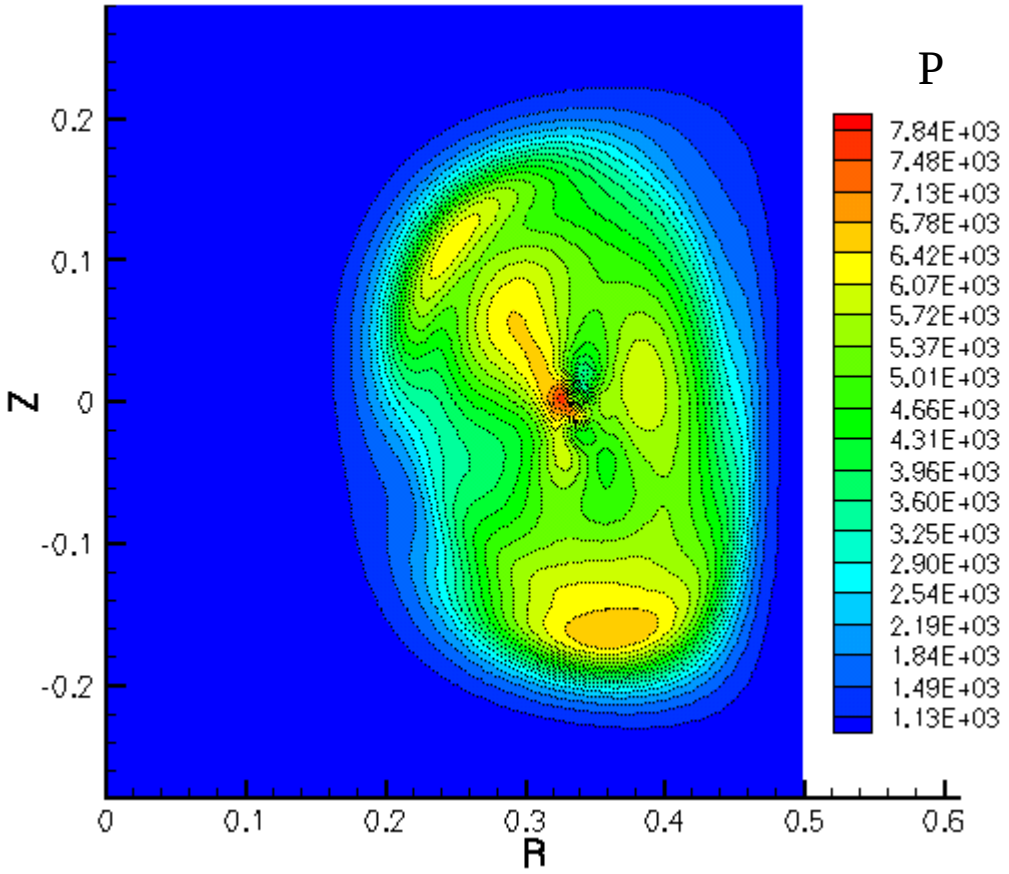

t=0.1348ms

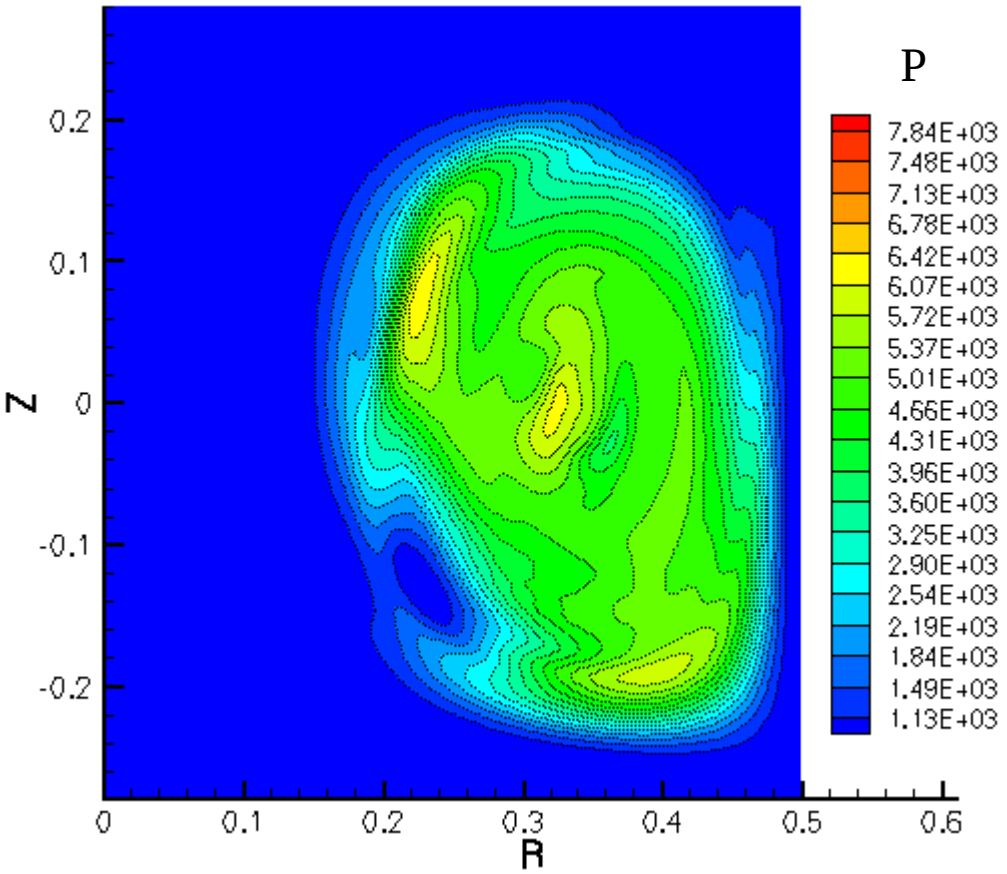

The closed flux surfaces in the lobes are destroyed and a new magnetic axis begins to form in two fluid simulations when the perturbed magnetic energy is small.

t=0.10089ms

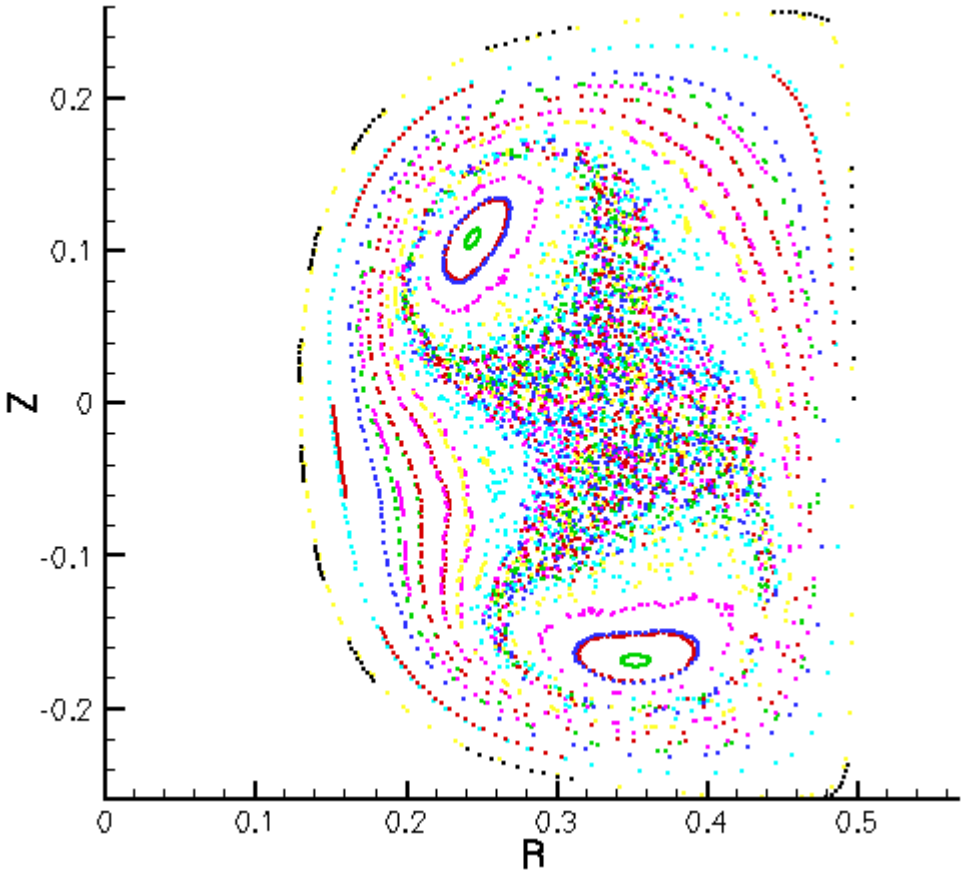

t=0.1348ms

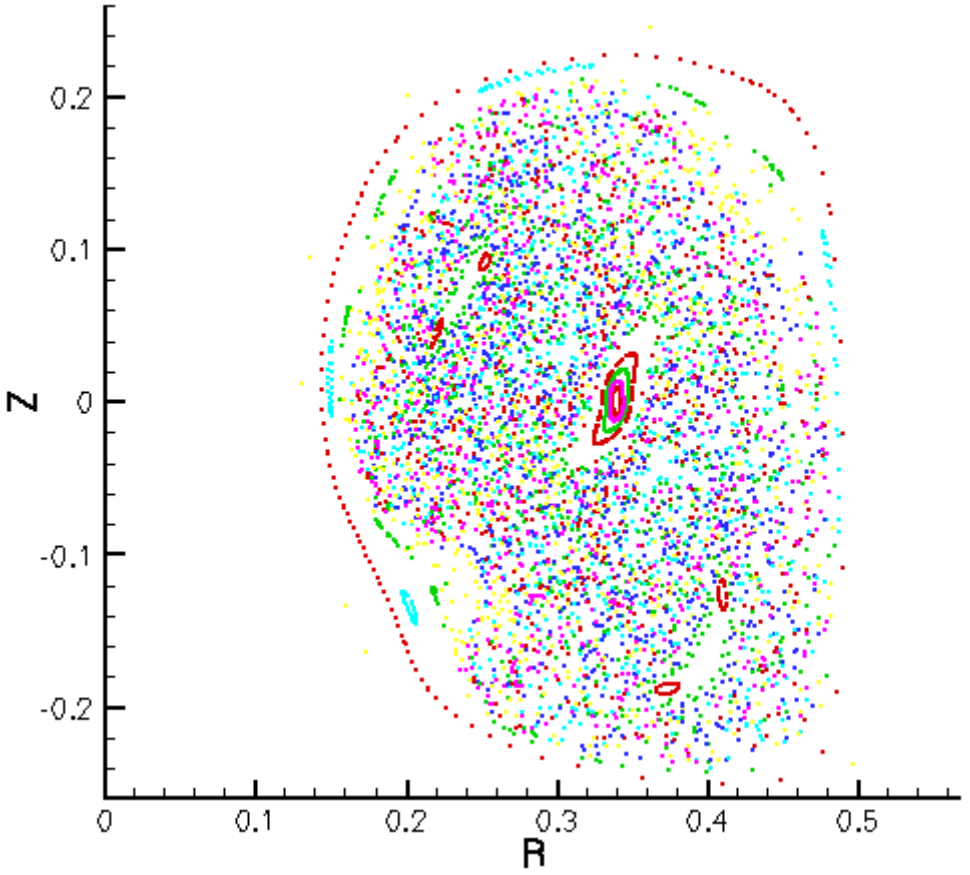

Conclusions

- Linear calculations of interchange modes have been performed for a linear spheromak and a realistic decaying spheromak equilibrium in a tuna-can geometry.
  - In the cylindrical spheromak equilibrium, the Hall physics is the dominate stabilizing mechanism for the resistive interchange mode, and the gyro-viscous stress is the dominate stabilizing mechanism for ideal interchange modes.
  - The Hall physics and the gyro-viscous stress have comparable effects on the growth rates of the n=3 and n=5 modes in the more realistic configuration.
- Nonlinear simulations of the interchange mode have been performed with the realistic spheromak equilibrium.
  - As the instability evolves two lobes of high pressure are formed near the edge, and the pressure in the core is reduced.
  - When two-fluid physics are included, the perturbed magnetic energy is reduced relative to the MHD result.